

Supporting information

Sacrificial Mo-S modification and P doping co-assisted activation strategy to enhance electrochemical performance of cobalt carbonate hydroxide hydrate

Ting Xiao^{*,a,b}, Zhixin Wang^a, Tao Jiang^a, Yushuai Yao^a, Lihua Jiang^b, Peng Xiang^b,
Shibing Ni^a, Weifeng Chen^a, Fujun Tao^c, Xinyu Tan^{*,a}

^a Key Laboratory of Inorganic Nonmetallic Crystalline and Energy Conversion Materials, College of Materials and Chemical Engineering, China Three Gorges University, Yichang, Hubei 443002, P. R. China

^b Hubei Provincial Engineering Technology Research Center for Microgrid, College of Electrical Engineering & New Energy, China Three Gorges University, Yichang, Hubei 443002, P. R. China

^c Department of Chemistry and Biochemistry, Northern Illinois University, DeKalb, IL 60115, USA

1. Experimental

* E-mail address: tingxiao@ctgu.edu.cn

* E-mail address: tanxin@ctgu.edu.cn

1.1 Raw material

$\text{Co}(\text{NO}_3)_2 \cdot 6\text{H}_2\text{O}$ ($\geq 98.5\%$) and urea ($\text{CH}_4\text{N}_2\text{O}$, $\geq 99\%$) were purchased from Sinopharm Chemical Reagent Co. Ltd. Ammonium molybdate ($(\text{NH}_4)_6\text{Mo}_7\text{O}_{24} \cdot 4\text{H}_2\text{O}$, $\geq 99.0\%$) was purchased from Sinopharm Chemical Reagent Co, Ltd. Ammonium fluoride (NH_4F , $\geq 98\%$) was purchased from Tianjin Zonghengxing Chemical Reagents Ltd. Thioacetamide (TAA) ($\text{C}_2\text{H}_5\text{NS}$, $\geq 99\%$) was supplied by Tianjin Tianli Chemical Reagents Ltd. Sodium hypophosphite (NaH_2PO_2 , 99.0%) and potassium hydroxide (KOH, 95%) come from Sinopharm Chemical Reagent Co, Ltd. Deionized (DI) water were used throughout all experiments.

Nickel foam (Purity: $\sim 99.99\%$, Porosity: $\geq 96.0\%$, Average hole diameters: ~ 0.25 mm, Surface density: $350 \pm 25 \text{ g/m}^2$) was obtained from Hefei Kejing Materials Technology Co. Ltd. CC (Surface density: $\sim 170 \text{ g m}^{-2}$) was supplied by Shanghai Lishuo Composite Materials Technology Co, Ltd.

1.2 Characterizations

Phase structure of the as-prepared products was characterized on Rigaku Ultima IV X-ray diffractometer with Cu Ka radiation ($\lambda = 1.5406 \text{ \AA}$). The morphology, lattice structure and element content of products was analyzed by scanning electron microscopy (SEM, Zeiss Gemini SEM 300), transmission electron microscope (TEM, Tecnai, G220 UTWIN) and HR-TEM (JEOL 2100F) with energy dispersive X-ray spectroscopy (EDX). X-ray photoelectron spectroscopy (XPS) analysis was realized on a PHI Quantera II X-ray photoelectron spectrometer. Brunauer-Emmett-Teller (BET, ASAP2460) was used to characterize the specific surface area of the materials.

Electrochemical analyses were carried out with a three-electrode on a CHI760E electrochemical workstation (Shanghai Chenhua Instrument Corp.) in 1 M KOH aqueous solution at room temperature. The as-prepared electrode (1 cm×1 cm), platinum plate electrode (1 cm×1 cm) and Hg/HgO (1M KOH) electrode were used as the working electrode, the counter electrode and the reference electrode, respectively. Electrochemical impedance spectroscopy (EIS) measurements were recorded at open-circuit potential in the frequency range of 100 kHz to 100 mHz. For the ASCs, two-electrode system was used with CCHH/Mo-S/P/A (1.0×1.0 cm²) as the cathode, commercial conductive carbon cloth (CC) (1.0×1.0 cm²) as the anode and 1 M KOH as electrolyte.

2. Electrochemical performance calculation:

Based on GCD curves, the areal capacities and specific capacities of the as-synthesized electrodes were calculated according to the equation S1 and S2, respectively:

$$Q_s = \frac{I \int_0^{\Delta t} V dt}{S \times \Delta V_{mean}} = \frac{I \int_0^{\Delta t} V dt}{S \times \frac{\Delta V}{2}} = 2 \frac{I \int_0^{\Delta t} V dt}{S \times \Delta V} \quad (S1)$$

$$Q_m = \frac{I \int_0^{\Delta t} V dt}{m \times \Delta V_{mean}} = \frac{I \int_0^{\Delta t} V dt}{m \times \frac{\Delta V}{2}} = 2 \frac{I \int_0^{\Delta t} V dt}{m \times \Delta V} \quad (S2)$$

where Q_s , Q_m , I , Δt , V , ΔV_{mean} , S , m , and ΔV are the areal capacity (C cm²), specific capacity (C g⁻¹), discharge current (A), discharge time (s), operating potential (V), mean value of operating potential (V), area of the device (cm²), mass (g), and potential window (V) of electroactive materials, respectively.

For the fabrication of ASC device, areal capacity (Q , $C \text{ cm}^{-2}$), energy density (E , $W \text{ h cm}^{-2}$) and power density (P , $W \text{ cm}^{-2}$) of device were calculated from current charging/discharging curves using the following equations, respectively.

$$Q = 2 \frac{I \int_0^{\Delta t_s} V_s dt}{S \times \Delta V_s}$$

$$E = \frac{I \int_0^{\Delta t_s} V_s dt}{3.6 \times S}$$

$$P = \frac{3600 \times E}{\Delta t_s}$$

where I , S , Δt_s , V_s and ΔV_s are the discharge current (A), area of the device (cm^2), discharge time (s), operating voltage (V), and voltage window (V) of the discharge process, respectively.

3. Supplementary figures and tables:

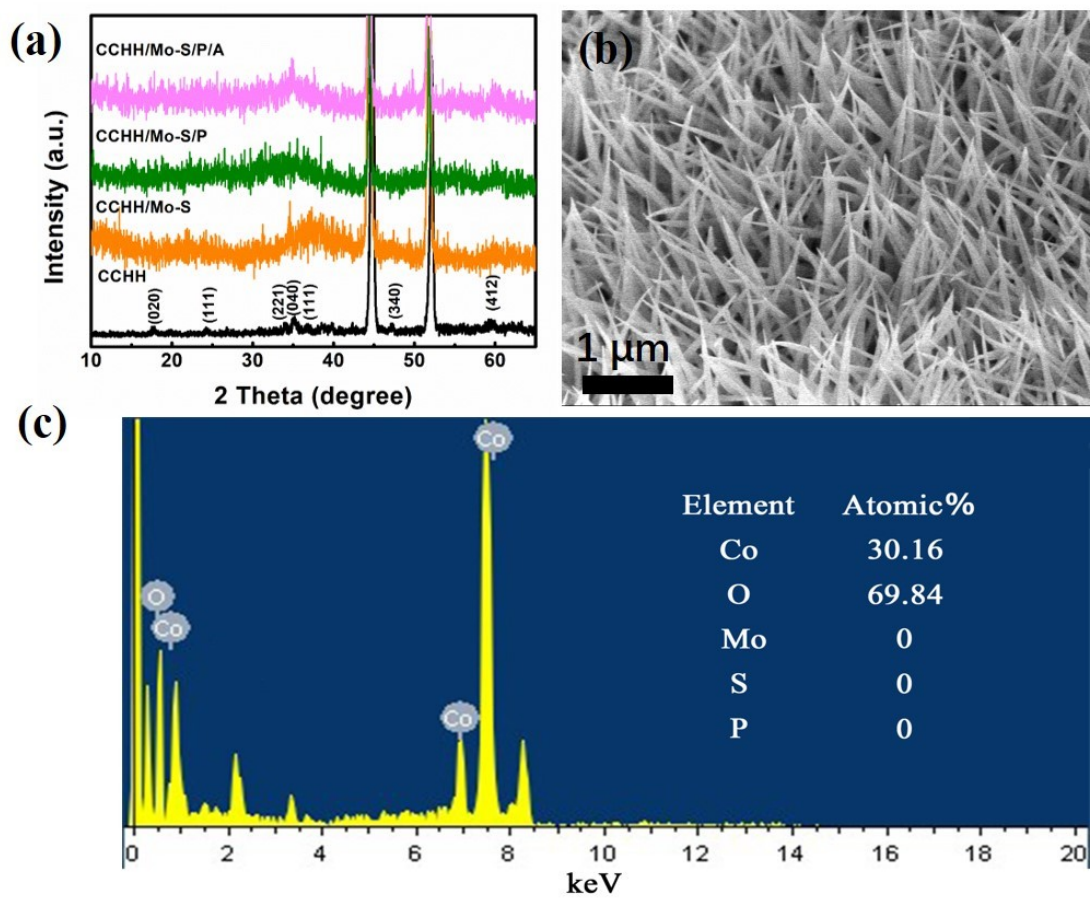


Fig. S1 (a) XRD patterns of the CCHH, CCHH/Mo-S, CCHH/Mo-S/P and CCHH/Mo-S/P/A. (b) SEM image of CCHH. (c) EDS data of the CCHH/Mo-S/P/A.

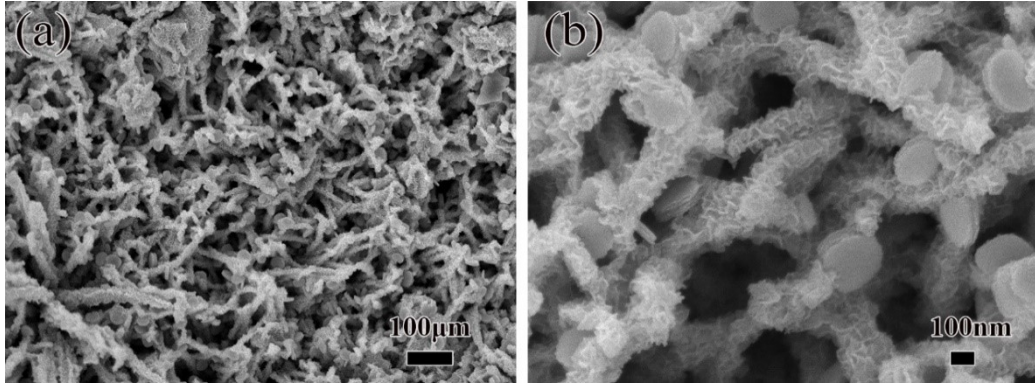


Fig. S2 SEM images of the CCHH/A at different magnifications.

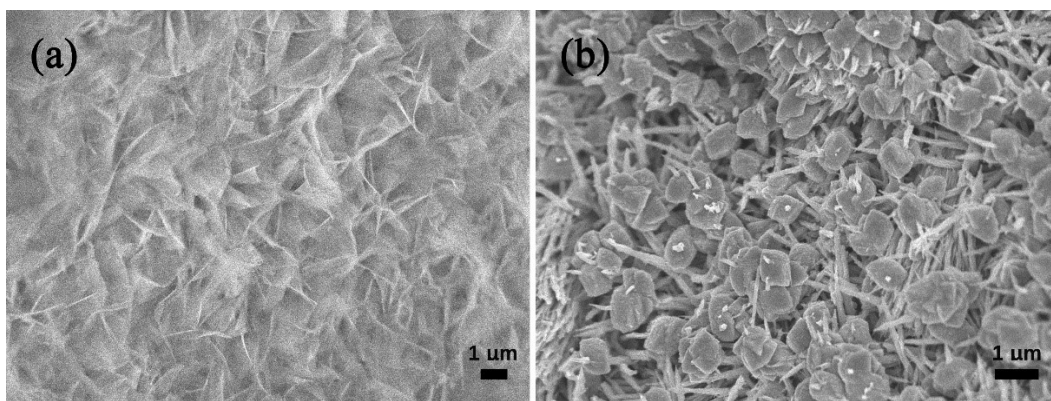


Fig. S3 (a) SEM image of CCHH/Mo-S/A. (b) SEM image of CCHH/P/A

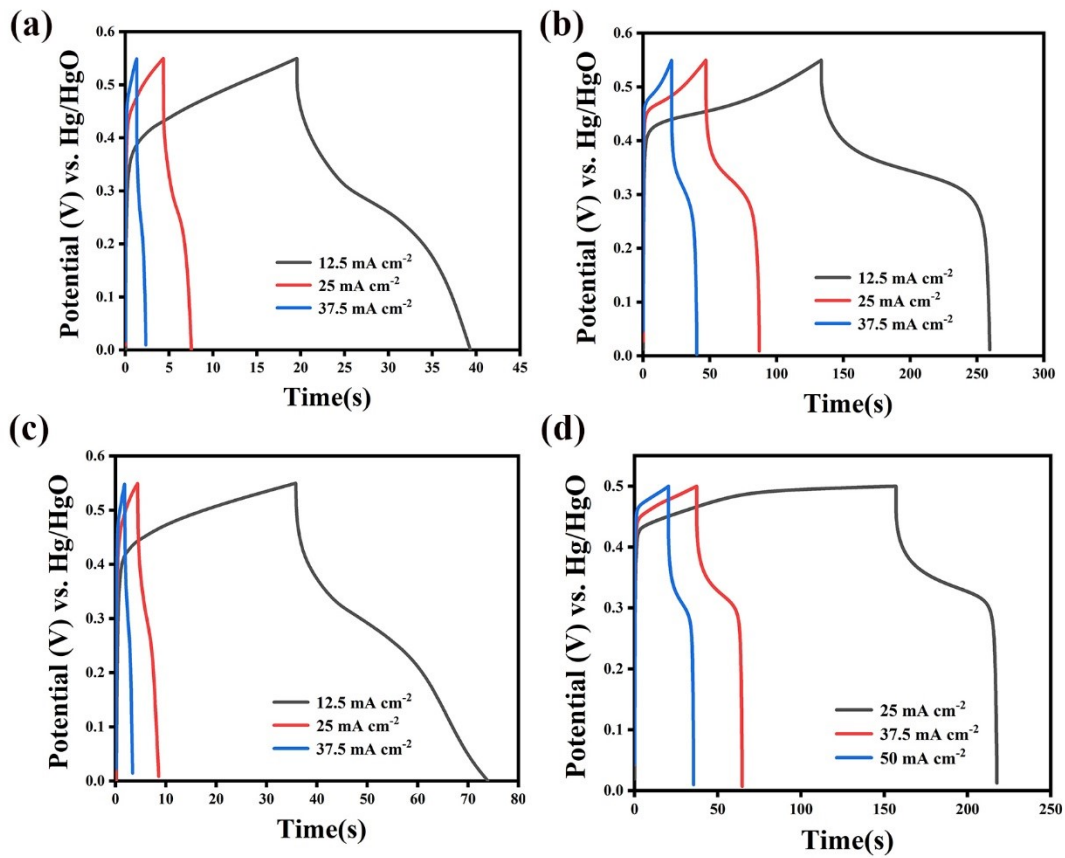


Fig. S4 GCD curves at different densities of the (a) CCHH/A, (b) CCHH/Mo-S/A, (c) CCHH/P/A and (d) CCHH/Mo-S/P.

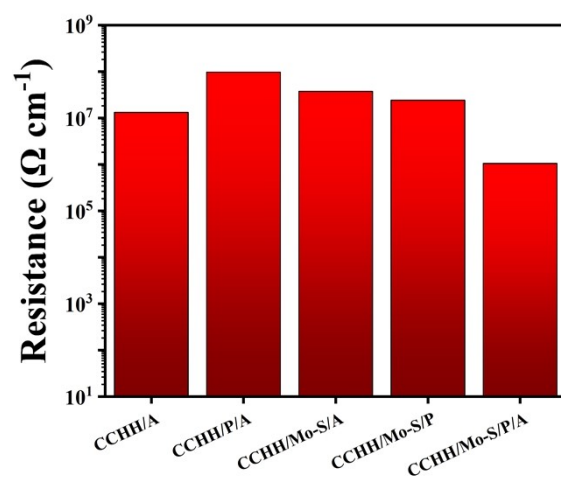


Fig. S5 Comparison of resistance for CCHH/A, CCHH/P/A, CCHH/Mo-S/A, CCHH/Mo-S/P and CCHH/Mo-S/P/A.

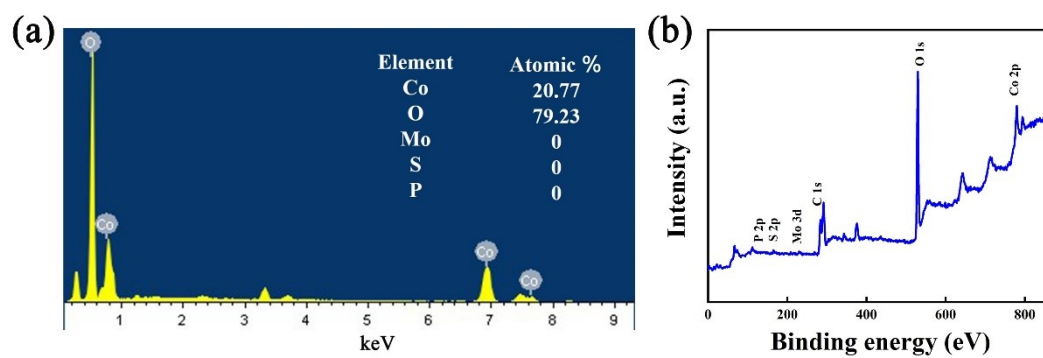


Fig. S6 (a) EDS data and (b) XPS survey spectra of the CCHH/Mo-S/P/A after 10000 cycles.

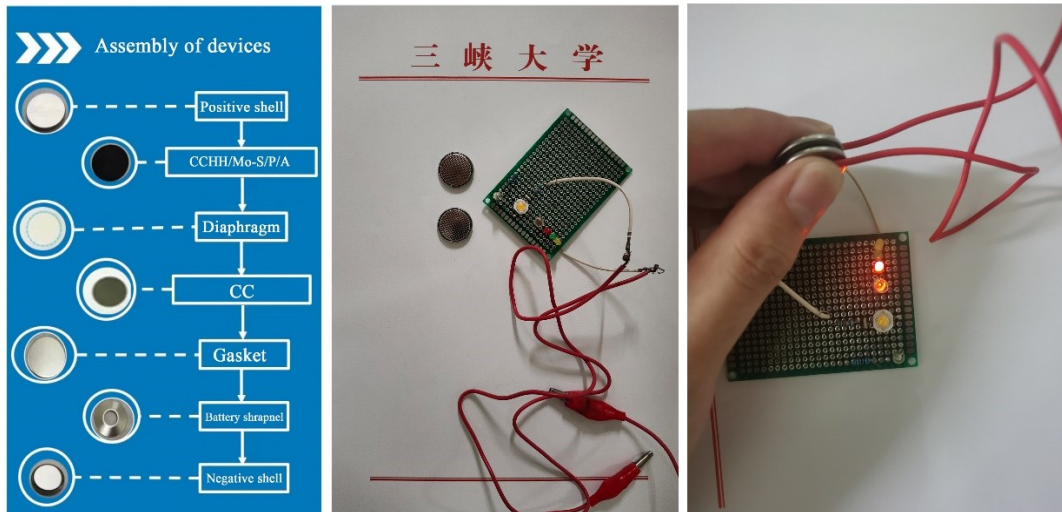


Fig. S7 CCHH/Mo-S/P/A//CC device assembly process and lighting LED indicator.

Table S1. Comparison of the specific capacitance between this work and several reports on Co-based binary metal electrode materials.

Materials	Electrolyte	Operation Voltage (V)	Specific capacitance	Current density	Ref.
FeCo ₂ S ₄	6 M KOH	0~0.4	1.644 F cm ⁻² (0.66 C cm ⁻²)	50 mA cm ⁻²	[20]
FeCo ₂ S ₄	1 M KOH	0~0.4	7.66 F cm ⁻² (3.06 C cm ⁻²)	5 mA cm ⁻²	[21]
Co-Mo-S	1 M KOH	0~0.45	1,080 F g ⁻¹ (468 C g ⁻¹)	1 A g ⁻¹	[22]
CoNi ₂ S ₄	6 M KOH	0~0.4	1,576.8 F g ⁻¹ (630.72 C g ⁻¹)	0.5 A g ⁻¹	[23]
NiCo ₂ S ₄	2 M KOH	0~0.45	1,777 F g ⁻¹ (799.65 C g ⁻¹)	8 A g ⁻¹	[24]
CuCo ₂ S ₄	4 M KOH	0~0.5	908.9 F g ⁻¹ (454.45 C g ⁻¹)	5 mA cm ⁻²	[25]
CuCo ₂ S ₄	2 M KOH	0~0.4	1,852 F g ⁻¹ (740.8 C g ⁻¹)	2 A g ⁻¹	[26]
CoMoS ₄	6 M KOH	0~0.45	415 F g ⁻¹ (186.75 C g ⁻¹)	0.5 A g ⁻¹	[27]
Co ₃ S ₄ /CoMo ₂ S ₄	3 M KOH	0~0.45	1,457.8 F g ⁻¹ (656 C g ⁻¹)	1 A g ⁻¹	[28]
Co-Mo-S	1 M KOH	0~0.5	1,805.28 F g ⁻¹ (902.64 C g ⁻¹)	0.5 A g ⁻¹	[29]
Co ₉ S ₈ @MoS ₂	1 M KOH	0~0.5	213 mAh g ⁻¹ 1,225 F g ⁻¹ (490 C g ⁻¹)	1 A g ⁻¹	[30]
Mo _{0.7} Co _{0.3} S ₂ -C ₃ N ₄	2 M KOH	0~0.4	1,145 F g ⁻¹ (458 C g ⁻¹)	0.5 A g ⁻¹	[31]
NiCo ₂ S ₄ @N, S	6 M KOH	0~0.4	1,454 F g ⁻¹ (727 C g ⁻¹)	1 A g ⁻¹	[32]
Ni-Co-S	1 M KOH	0~0.5	1,440 C g ⁻¹ (720 C g ⁻¹)	1 A g ⁻¹	[33]
Ni-Co-S/Co(OH) ₂	3 M KOH	0~0.5	1,158 F g ⁻¹ (521.1 C g ⁻¹)	1 A g ⁻¹	[34]
Mn-Co-S	1 M KOH	0~0.45	1,134 F g ⁻¹ (396.9 C g ⁻¹)	1 A g ⁻¹	[35]
Co-Mo-O-S	6 M KOH	0~0.35	1,437.5 F g ⁻¹ (862.5 C g ⁻¹)	1 A g ⁻¹	[36]
Co-Mo-O	3 M KOH	0~0.6	879 F g ⁻¹ (307.65 C g ⁻¹)	1.5 A g ⁻¹	[37]
NiCo ₂ O ₄	2 M KOH	0~0.35		0.5 A g ⁻¹	[38]

CCHH/Mo-S/P/A	1 M KOH	0~0.55	1429 C g ⁻¹ (4.29 C cm ⁻²)	12.5 mA cm ⁻² (4.2 A g ⁻¹)	This work
---------------	---------	--------	--	--	--------------
